Pure Silica Zeolite-type Frameworks: A Structural Analysis

David S. Wragg,*,‡ Russell E. Morris,‡ and Allen W. Burton†

EaStChem School of Chemistry, University of St. Andrews, St. Andrews, Fife, KY16 9ST United Kingdom, and Chevron Energy Technology Company, 100 Chevron Way, Richmond, California 94802

Received July 11, 2007. Revised Manuscript Received October 11, 2007

Since the last major study of silicate crystal structures, many new pure silica zeolite-type frameworks have been discovered. These materials have many interesting properties that are dependent on their structure. We have brought together and analyzed the structures in 35 well-defined frameworks to see how they differ from one another depending on the synthetic route, template, calcination, and composition, and how they differ from the dense silicate phases previously examined. The grand mean values of the Si−O bond distance and the O−Si−O angle are found to be 1.594 Å and 109.5°, respectively. The variation and flexibility of the Si−O−Si bond from 133.6 to 180° is discussed, as is the role of fluoride in influencing the O−Si−O bond angles in phases prepared using hydrofluoric acid and ammonium fluoride as mineralizers.

Introduction

The properties of framework materials like zeolites are intimately linked to their structure. Their tremendous usefulness in catalysis, separation, adsorption, ion exchange, and drug delivery and as templates for new materials and low-*k* dielectrics for microprocessors comes directly from their channels, pores, and pockets.[1–4] These of course depend on the bonding and makeup of the solids. Pure silica zeolites (PSZ) are a particularly interesting group being highly thermally stable, structurally diverse, chemically simple (silica polymorphs), and closely related to catalytically interesting materials. Many of these have been well-characterized by single-crystal and powder diffraction techniques. Several reviews[5–7] have been devoted to the synthesis of these materials, yet the latest analysis of crystal structural data (for the silica polymorphs in general) is that of Liebau from 1985.[8] Here, we present an analysis of the currently available structural data for PSZ and compare them to those of other silica polymorphs so that the data may be used to help explain the fascinating properties of these materials. We hope that bringing all of these data together in a single publication will prove helpful to researchers in this area. Since the Liebau study, a much larger number of PSZ have been made; in fact, most of the materials analyzed before were dense phases or clathrasils. The clathrasils, having framework structures similar to zeolites, are also included in our analysis.

Like most silicates, a PSZ is built of SiO_4 tetrahedra. There is a rich variety in how these tetrahedra link together to form the many different possible framework structures. The way the connectivity of tetrahedra varies and how this affects the Si−O bonds, Si−O−Si and O−Si−O angles, and their value ranges are of great interest. Are they any different from those of dense silicates?

For the purposes of this analysis, we have adopted Liebau's standard of a crystallographic *R* factor[9] of 8% or less for a structure determined from single-crystal diffraction data to be considered well-defined.[8] Because of the difficulty in growing large enough crystals, many PSZ structures have been determined from powder X-ray diffraction (XRD) data and refined using the Rietveld method.[10] The commonly reported R_{wp} and R_p agreement values for such refinements are poor indicators of structure quality,[11] especially in cases in which geometric restraints are used. We have therefore included in our overall analysis only structures for which the Rietveld refinement converged without restraints on either bond lengths or angles. In all the structures rejected, the authors reported that the restraints were necessary for completion of the refinement. Interestingly, our analysis shows very little difference in averages between the highly reliable single-crystal data and the unrestrained powder refinements.

The crystal structures of 38 PSZs have been described in the literature (see Table 1). We have analyzed the data for 41 well-defined crystal structures that meet the above criteria (24 different PSZ topologies[72]). All data sets that meet the

* Corresponding author. E-mail: dsw@st-andrews.ac.uk.
‡ University of St. Andrews.
† Chevron Energy Technology Company.

(1) Davis, M. E. *Nature* **2002**, *417*, 813–821.
(2) Wheatley, P. S.; Butler, A. R.; Crane, M. S.; Fox, S.; Xiao, B.; Rossi, A. G.; Megson, I. L.; Morris, R. E. *J. Am. Chem. Soc.* **2006**, *128*, 502–509.
(3) Schüth, F. *Angew. Chem., Int. Ed.* **2003**, *42*, 3604–3622.
(4) Wang, Z. B.; Mitra, A. P.; Wang, H. T.; Huang, L. M.; Yan, Y. S. *Adv. Mater.* **2001**, *14*, 1463.
(5) Villaescusa, L. A.; Camblor, M. A. *Recent Res. Dev. Chem.* **2003**, *1*, 93–141.
(6) Camblor, M. A.; Villaescusa, L. A.; Díaz-Cabañas, M. J. *Top. Catal.* **1999**, *9*, 59–76.
(7) Caullet, P.; Paillaud, J-L.; Simon-Masseron, A.; Soulard, M.; Patarin, J. *C.R. Chim.* **2005**, *8*, 245–266.
(8) Liebau, F. *Structural Chemistry Of Silicates: Structure, Bonding, and Classification*; Springer-Verlag: Berlin, 1985; pp 14–30.
(9) Viterbo, D. In *Fundamentals of Crystallography*, 1st ed.; Giacovazzo, C., Ed.; Oxford University Press/IUCr: Oxford, U.K., 1992; pp 319–401. Note that *R* factors reported here are for "observed" data. The observed criteria differ slightly from one paper to another and can be found therein by readers who are worried about them.
(10) Rietveld, H.M. J. *Appl. Crystallogr.* **1969**, *2*, 65–71.
(11) Hill, R. J.; Fischer, R. X. *J. Appl. Crystallogr.* **1990**, *23*, 462–468.

10.1021/cm071824j CCC: $40.75 © 2008 American Chemical Society
Published on Web 01/17/2008

Table 1. Pure Silica Zeolite Type Structures Currently Available

pure silica material	framework code	calcination status	R/R_{wp} (R_{exp})[a]	restraints used?	data type	analyzed?	ref
SSZ-24	**AFI**	as-made	0.145(0.035)	no	P	yes	12
SSZ-24	**AFI**	calcined	0.158(0.036)	no	P	yes	12
octadecasil	**AST**	as-made	0.0613	no	SC	yes	13
SSZ-55[d]	**ATS**	as-made	0.0388	no	SC	yes	14
zeolite beta	**BEA**	NA	NA	NA	model	no	15
ITQ-14	**BEC**	NA	NA	NA	model	no	16
CIT-5	**CFI**	calcined	0.0709	yes	P	no	17
CIT-5	**CFI**	calcined	0.0949	yes	P	no	18
chabazite	**CHA**	calcined	0.1118(0.0776)	no	P	yes	19
chabazite	**CHA**	as-made	0.058	no	SC	yes	20
chabazite	**CHA**	calcined	0.0544	no	SC	yes	21
deca-dodecasil	**DDR**	as-made	0.167	no	SC	no	22
dodecasil-1H	**DOH**	as-made	0.056	no	SC	yes	23
UTD-1	**DON**	NA	NA	NA	model	no	24
EU-1	**EUO**	calcined	NA	yes	P	no	25
dealuminated zeolite-Y	**FAU**	calcined	0.0309(0.0216)	no	P[c]	yes	26
ferrierite	**FER**	as-made	0.0312	no	SC	yes	27
FER as-made	**FER**	as-made	0.0465	no	SC	yes	20
FER calcined	**FER**	calcined	0.0513	no	SC	yes	28
GUS-1	**GON**	calcined	0.074	yes	P	no	29
SSZ-42	**IFR**	calcined	0.066(0.065)	no	SC/P[e]	yes	30
ITQ-4	**IFR**	calcined	0.0767(0.042)	no	P	yes	31
ITQ-4	**IFR**	as made	0.045, 0.048, 0.0525	no	SC	yes	32–34
ITQ-4	**IFR**	calcined	0.0578	no	SC	yes	34
ITQ-32	**IHW**	calcined	0.052(0.033)	yes	P	no	35
ITQ-7	**ISV**	calcined	0.1076(0.063)	no	P	yes	36
ITQ-3	**ITE**	calcined	0.086	yes	P	no	37
ITQ-13	**ITH**	as-made	0.08	no	SC	yes	38
ITQ-12	**ITW**	calcined	0.1439(0.0423)	yes	P	no	39
ITQ-12	**ITW**	as-made	0.055(0.009)	yes	P	no	40
ITQ-12	**ITW**	calcined	0.056(0.009)	yes	P	no	40
ITQ-24	**IWR**	calcined	0.12(0.041)	Yes[I]	P	yes	41
ITQ-29	**LTA**	calcined	0.097(0.058)	no	P	yes	42
ZSM-11	**MEL**	calcined	0.13[j]	no	P	yes	43
ZSM-11	**MEL**	calcined	0.0748(0.0390)	no	P	yes	44
ZSM-11	**MEL**	as-made	0.064	no	SC	yes	45,46[h]
silicalite, ZSM-5	**MFI**	as-made	0.042	no	SC	yes	47
silicalite, ZSM-5 (fluoride version)	**MFI**	as-made	0.036	no	SC	yes	48
MCM-35	**MTF**	calcined	0.0916(0.0612)	no	P	yes	49
ZSM-39, dodecasil-3c	**MTN**	as-made	0.034	no	SC	yes	50
ZSM-39, dodecasil-3c, CF-4	**MTN**	as-made	0.055	no	SC	yes	51
ZSM-39, dodecasil-3c	**MTN**	as-made	0.039	no	SC	yes	52
ZSM-23	**MTT**	calcined[g]	0.085(0.033)	yes	P	no	53
ZSM-12	**MTW**	calcined	0.181(0.058)	no	P	yes	54
ZSM-12	**MTW**	calcined[f]	0.084(0.083)	no	P	yes	55
ITQ-1, MCM-22, SSZ-25	**MWW**	calcined	0.159(0.103)	yes	P	no	56
nonasil	**NON**	as-made	0.047	no	SC	yes	57
RUB-41	**RRO**	calcined	0.089(0.059)	yes	P	no	58
RUB-3	**RTE**	as-made	0.099	no	SC	no	59
RUB-3	**RTE**	calcined	0.073(0.057)	yes	P	no	59
RUB-10	**RUT**	as-made	0.12(0.119)	no	P	yes	60
RUB-24	**RWR**	calcined	0.106(0.061)	yes	P	no	61
SSZ-73*	**SAS**	as-made	0.15	no	SC	no	62
SSZ-73	**SAS**	calcined	0.1224(0.056)	no	P	yes	62
sigma-2	**SGT**	as-made	0.225(0.190)	no	P	yes	63
sodalite trioxane	**SOD**	as-made	0.077(0.11)	no	P[c]	yes	64
sodalite ethylene glycol	**SOD**	as-made	0.024	no	SC	yes	65
sodalite ethylene glycol	**SOD**	as-made	0.013	no	P[c]	yes	65
SSZ-31	**NA**	NA	NA	NA	model	no	64
SSZ-35, ITQ-9, MU-26	**STF**	as-made	0.094	no	SC	no	32
SSZ-35, ITQ-9, MU-26	**STF**	as-made	0.0708	no	SC	yes	67
SSZ-35, ITQ-9, MU-26[d]	**STF**	as-made	0.0607	no	SC	yes	68
SSZ-23	**STT**	as-made	0.0811	no	SC	yes	69
SSZ-23	**STT**	calcined	0.0935	yes	P	no	70
theta-1	**TON**	calcined	0.08	no	SC	yes	71

[a] The R value is given for structures determined from single-crystal XRD data and R_{wp} (followed in brackets by R_{exp} if available) where powder data were used. [b] SC = Single-crystal X-ray data; P = powder X-ray data (except when marked with footnote c). [c] Neutron data. [d] Electron density from pores removed using the SQUEEZE algorithm. [e] Single-crystal structure used for Rietveld refinement against powder data. [f] Adsorbed with 4-nitroaniline. [g] Adsorbed with ammonium fluoride. [h] Unit-cell data from ref 43. [I] Restraints on thermal parameters, not bond lengths/angles. [j] R_p used, as R_{wp} was not given.

"well-defined" criteria are included in our analysis, and curious features of the different determinations are discussed. During this work, we also improved the refinement of framework single-crystal X-ray data for ITQ-9, the pure silica form of the **STF** zeolite topology, to meet Liebau's well-defined criterion. These new data are included in our analysis.

We have relaxed the strict 8% for two structures whose *R* factors fall just below this standard; they are included because they fit well inside the patterns seen for the other materials and represent the best data likely to be found for these structures. The data used in the analysis were supplied by the UK Chemical Database Service[73] from the Cambridge Structural Database[74] or from the Supporting Information published with the cited papers.

PSZs are normally synthesized in the presence of organic structure-directing agents (SDAs).[5–7] It is desirable to determine the structure with the SDA present in order to study its orientation in the framework. This makes the already complicated zeolite structure more complex still, and in some cases, it is not possible to locate all the atoms in both framework and SDA. For many early structure determinations, especially those from powder diffraction data, the SDA was either ignored or removed prior to data collection by calcination (heating to decompose and drive out the organic molecules). Sometimes, even with single-crystal data, the position of the SDA cannot be determined because of

(12) Bialek, R.; Meier, W. M.; Davis, M.; Annen, M. J. *Zeolites* **1991**, *11*, 438–442.
(13) Caullet, P.; Guth, J. L.; Hazm, J.; Lamblin, J. M.; Gies, H. *Eur. J. Solid State Inorg. Chem.* **1991**, *28*, 345–361.
(14) Burton, A.; Darton, R. J.; Davis, M. E.; Hwang, S.; Morris, R. E.; Ogino, I.; Zones, S. I. *J. Phys. Chem. B* **2006**, *110*, 5273–5278.
(15) Camblor, M. A.; Corma, A.; Valencia, S. *J. Chem. Soc., Chem. Commun.* **1996**, 2365–2366.
(16) Liu, Z.; Ohsuna, T.; Terasaki, O.; Camblor, M. A.; Diaz-Cabañas, M.-J.; Hiraga, K. *J. Am. Chem. Soc.* **2001**, *123*, 5370–5371.
(17) Yoshikawa, M.; Wagner, P.; Lovallo, M.; Tsuji, K.; Takewaki, T.; Chen, C.-Y.; Beck, L. W.; Jones, C.; Tsapatsis, M.; Zones, S. I.; Davis, M. E. *J. Phys. Chem. B* **1998**, *102*, 7139–7147.
(18) Barrett, P. A.; Díaz-Cabañas, M.-J.; Camblor, M. A.; Jones, R. H. *J. Chem. Soc., Faraday Trans.* **1998**, *94*, 2475–2481.
(19) Díaz-Cabañas, M.-J.; Barrett, P. A.; Camblor, M. A. *J. Chem Soc., Chem. Commun.* **1998**, 1881–1882.
(20) Villaescusa, L. A.; Bull, I.; Wheatley, P. S.; Lightfoot, P.; Morris, R. E. *J. Mater. Chem.* **2003**, *13*, 1978–1982.
(21) Villaescusa, L. A.; Bull, I.; Wheatley, P. S.; Lightfoot, P.; Morris, R. E. Unpublished data.
(22) Gies, H. *Z. Kristallogr.* **1986**, *175*, 93–104.
(23) Gerke, H.; Gies, H. *Z. Kristallogr.* **1984**, *166*, 11–22.
(24) Lobo, R. F.; Tsapatsis, M.; Freyhardt, C. C.; Khodabandeh, S.; Wagner, P.; Chen, C-Y., Jr.; Zones, S. I.; Davis, M. E. *J. Am. Chem. Soc.* **1997**, *119*, 8474–8484.
(25) Briscoe, N. A., Jr.; Shannon, M. D.; Kokotailo, G. T.; McCusker, L. B. *Zeolites* **1988**, *8*, 74–76.
(26) Hriljac, J. A.; Eddy, M. M.; Cheetham, A. K.; Donohue, J. A.; Ray, G.J. J. *Solid State Chem.* **1993**, *106*, 66–72.
(27) Weigel, S. J.; Gabriel, J-C.; Gutierrez-Puebla, E.; Monge Bravo, A.; Henson, N. J.; Bull, L. M.; Cheetham, A. K. *J. Am. Chem. Soc.* **1996**, *118*, 2427–2435.
(28) Bull, I.; Lightfoot, P.; Villaescusa, L. A.; Bull, L. M.; Gover, R. K. B.; Evans, J. S. O.; Morris, R. E. *J. Am. Chem. Soc.* **2003**, *125*, 4342–4349.
(29) Plévert, J.; Kubota, Y.; Honda, T.; Okuboa, T.; Sugib, Y. *Chem. Commun.* **2000**, 2363–2364.
(30) Chen, C.-Y.; Finger, L. W.; Medrud, R. C.; Crozier, P. A.; Chan, I. Y.; Harris, T. V.; Zones, S. I. *J. Chem. Soc., Chem. Commun.* **1997**, 1775–1776.
(31) Barrett, P. A.; Camblor, M. A.; Corma, A.; Jones, R. H.; Villaescusa, L. A. *Chem. Mater.* **1997**, *9*, 1713–1715.
(32) Bull, I.; Villaescusa, L. A.; Teat, S. J.; Camblor, M. A.; Wright, P. A.; Lightfoot, P.; Morris, R. E. *J. Am. Chem. Soc.* **2000**, *122*, 7128–7129.
(33) Villaescusa, L. A.; Wheatley, P. S.; Bull, I.; Lightfoot, P.; Morris, R. E. *J. Am. Chem. Soc.* **2001**, *123*, 8797–8805.
(34) Villaescusa, L. A.; Lightfoot, P.; Teat, S. J.; and Morris, R. E. *J. Am. Chem. Soc.* **2001**, *123*, 5453–5459.
(35) Cantín, A.; Corma, A.; Leiva, S.; Rey, F.; Rius, J.; Valencia, S. *J. Am. Chem. Soc.* **2005**, *127*, 11560–11561.
(36) Villaescusa, L. A.; Barrett, P. A.; Camblor, M. A. *Angew. Chem., Int. Ed.* **1999**, *38*, 1997–2000.
(37) Camblor, M. A.; Corma, A.; Lightfoot, P.; Villaescusa, L. A.; Wright, P. A. *Angew. Chem., Int. Ed.* **1997**, *23*, 2659–2661.
(38) Corma, A.; Puche, M.; Rey, F. *Angew. Chem., Int. Ed.* **2003**, *42*, 1156–1159.
(39) Barrett, P. A.; Boix, T.; Puche, M.; Olson, D. H.; Jordan, E.; Koller, H.; Camblor, M. A. *J. Chem. Soc., Chem. Commun.* **2003**, 2114–2115.
(40) Yang, X; Camblor, M. A.; Lee, Y.; Liu, H.; Olson, D. H. *J. Am. Chem. Soc.* **2004**, *126*, 10403–10409.
(41) Cantín, A.; Corma, A.; Diaz-Cabanas, M. J.; Jordá, J. L.; Moliner, M. *J. Am. Chem. Soc.* **2006**, *128*, 4216–4217.
(42) Corma, A.; Rey, F.; Rius, J.; Sabater, M. J.; Valencia, S. *Nature* **2004**, *431*, 287–290.
(43) Fyfe, C. A.; Gies, H.; Kokotailo, G. T.; Pasztor, C.; Strobl, H.; Cox, D. E. *J. Am. Chem. Soc.* **1989**, *111*, 2470–2474.
(44) Terasaki, O.; Ohsuna, T.; Sakuma, H.; Watanabe, D.; Nakagawa, Y.; Medrud, R. C. *Chem. Mater.* **1996**, *8*, 463–468.
(45) Van Koningsveld, H.; Den Exter, M. J.; Koegler, J. H.; Laman, C. D.; Njo, S. L.; Gaafsma, H. In *Proceedings of the 12th International Zeolite Conference*,Baltimore, MD, July 1998; Treacy, M. M. J., Marcus, B. K., Bisher, M. E., Higgins, J. B., Eds.; Materials Research Society: Warrendale, PA, 1999; pp 24192424
(46) Baur, W. H.; Fischer, R. X. In *Zeolite-Type Crystal Structures and Their Chemistry. Framework Type Codes DAC to LOV*; Subvolume C in Landolt−Börnstein, Group IV, Volume 14, Microporous and other framework materials with zeolite-type structures; Baur, W. H., Fischer, R. X., Eds.; Springer-Verlag: Berlin, 2002; p 459.
(47) Van Koningsveld, H.; Van Bekkum, H.; Jansen, J. C. *Acta Crystallogr, Sect. B* **1987**, *43*, 127–132.
(48) Aubert, E.; Porcher, F.; Souhassou, M.; Petøíček, V.; Lecomte, C. *J. Phys. Chem. B* **2002**, *106*, 1110–1117.
(49) Barrett, P. A.; Díaz-Cabañas, M.-J.; Camblor, M. A. *Chem. Mater.* **1999**, *11*, 2919–2927.
(50) Knorr, K.; Depmeier, W. *Acta Crystallogr., Sect. B* **1997**, *53*, 18–24.
(51) Long, Y.; He, H.; Zheng, P.; Wu, G.; Wang, B. J. *Inclusion Phenom.* **1987**, *5*, 355–362.
(52) Chae, H. K.; Klemperer, W. G.; Payne, D. A.; Suchicital, C. T. A.; Wake, D. R.; Wilson, S. R. *ACS Symp. Ser.* **1991**, *455*, 528–540.
(53) Marler, B.; Deroche, C.; Gies, H.; Fyfe, C. A.; Grondey, H.; Kokotailo, G. T.; Feng, Y.; Ernst, S.; Weitkamp, J.; Cox, D.E. J. *Appl. Crystallogr.* **1993**, *26*, 636–644.
(54) Fyfe, C. A.; Gies, H.; Kokotailo, G. T.; Marler, B.; Cox, D. E. *J. Phys. Chem.* **1990**, *94*, 3718–3721.
(55) Kinski, I.; Daniels, P.; Deroche, C.; Marler, B.; Gies, H. *Microporous Mesoporous Mater.* **2002**, *56*, 11–25.
(56) Camblor, M. A.; Corma, A.; Díaz-Cabañas, M.-J.; Baerlocher, Ch. *J. Phys. Chem. B* **1998**, *102*, 44–51.
(57) Van de Goor, G.; Freyhardt, C. C.; Behrens, P. *Z. Anorg. Allg. Chem.* **1995**, *621*, 311–322.
(58) Wang, Y. X.; Gies, H.; Marler, B.; Mueller, U. *Chem. Mater.* **2005**, *17*, 43–49.
(59) Marler, B.; Grunewald-Luke, A.; Gies, H. *Microporous Mesoporous Mater.* **1998**, *26*, 49–59.
(60) Marler, B.; Werthmann, U.; Gies, H. *Microporous Mesoporous Mater.* **2001**, *43*, 329–340.
(61) Marler, B.; Stroter, N.; Gies, H. *Microporous Mesoporous Mater.* **2005**, *83*, 201–211.
(62) Wragg, D. S.; Morris, R. E.; Burton, A. W.; Zones, S. I.; Ong, K.; Lee, G. *Chem. Mater.* **2007**, *19*, 3924–3932.
(63) McCusker, L.B. J. *Appl. Cryst.* **1988**, *21*, 305–310.
(64) Fuetterer, K.; Depmeier, W.; Altdorfer, F.; Behrens, P.; Felsche, J. *Z. Kristallogr.* **1994**, *209*, 517–523.
(65) Richardson, J. W. Jr.; Pluth, J.J.; Smith, J.V.; Dytrych, W.J.; Bibby, D.M. *J. Phys. Chem.* **1988**, *92*, 243–247.
(66) Lobo, R. F.; Tsapatsis, M.; Freyhardt, C. C.; Chan, I.; Chen, C-Y.; Zones, S. I.; Davis, M. E. *J. Am. Chem. Soc.* **1997**, *119*, 3732–3744.
(67) Fyfe, C. A.; Brouwer, D. H.; Lewis, A. R.; Villaescusa, L.A.; Morris, R. E. *J. Am. Chem. Soc.* **2002**, *124*, 7770–7778.
(68) Data in this study, see text and the Supporting Information.
(69) Camblor, M. A.; Díaz-Cabañas, M.-J.; Perez-Pariente, J.; Teat, S. J.; Clegg, W.; Shannon, I. J.; Lightfoot, P.; Wright, P. A.; Morris, R. E. *Angew. Chem., Int. Ed.* **1998**, *37*, 2122–2126.
(70) Camblor, M. A.; Díaz-Cabañas, M.-J.; Cox, P. A.; Shannon, I. J.; Wright, P. A.; Morris, R. E. *Chem. Mater.* **1999**, *11*, 2878–2885.
(71) Papiz, M. Z.; Andrews, S. J.; Damas, A. M.; Harding, M. M.; Highcock, R. M. *Acta Crystallogr., Sect. C* **1990**, *46*, 172–173.
(72) Baerlocher, Ch.; McCusker, L. B. Database of Zeolite Structures. http://www.iza-structure.org/databases/.
(73) Fletcher, D. A.; McMeeking, R. F.; Parkin, D. J. *Chem. Inf. Comput. Sci.* **1996**, *36*, 746–749.
(74) Allen, F. H. *Acta Crystallogr., Sect. B* **2002**, *58*, 380–388.

disorder. Recently, it has become computationally possible (and considered acceptable) to remove electron density from unmodeled disorder of SDA molecules in the pores of zeolites using the SQUEEZE algorithm (from Spek's PLATON crystallographic tool[75]).

Where available, we have included data for both the calcined and "as-made" (SDA included) structures and will present analysis for both types. In some cases, particularly the ITQ-*n* and SSZ-*n*[76] series of materials, PSZs are synthesized in the presence of fluoride. This complicates the structure again, as fluorine atoms are incorporated in different ways, with different effects on the bond lengths and angles. Furthermore, fluoride sites are often fractionally occupied so their effects on their nearest silicon sites are not uniform. Calcination removes the fluoride from the structure along with the SDA. Clearly, the as-made structures and those with fluorine directly bonded to silicon are not strictly PSZs, so we will discuss them separately. Where fluorine is present and may affect the measured bond lengths and angles, it has been excluded from the calculation of the averages and ranges.

The use of synchrotron radiation in single-crystal X-ray diffraction has proved exceptionally worthwhile for determining PSZ structures. Hydrothermal synthesis often produces microcrystalline powders rather than the nice, large single crystals favored by crystallographers. The tiny zeolite crystals give little or no diffraction when probed with X-rays from conventional laboratory sources, but can give useable data when high-intensity synchrotron X-rays are used. As early as 1990 Papiz and co-workers reported the redetermination of the theta-1 zeolite structure using single-crystal synchrotron data,[71] and recently, Morris et al. have published a series of PSZ structures and variable-temperature studies[14,20,21,28,32–34,62,67–69] from data collected at the dedicated microcrystal diffraction facility, station 9.8, of the SRS in Daresbury, U.K.[77]

Discussion

Si−O Bond Lengths. The bond lengths in the selected structures range from 1.540(9) Å (in the calcined MCM-35 structure[49]) to 1.67 Å (found in several structures). The grand mean value of the analyzed bond lengths is 1.597 ± 0.026 Å, for the room temperature data only the mean is slightly shorter at 1.594 ± 0.027 Å. The grand mean value corresponds to a peak in the distribution graph of the bond distances (Figure 1).

This mean value is essentially the same for all types of data (calcined, as-made, powder, single crystal, with and without restraints) and is not greatly affected by temperature. Liebau reports a grand mean value of 1.62 Å for all silica polymorphs, but a value of 1.608 Å for materials with an oxygen coordination number of 2. This compares well with the value of 1.609 Å predicted by eq 1 proposed by Brown and Gibbs.[78]

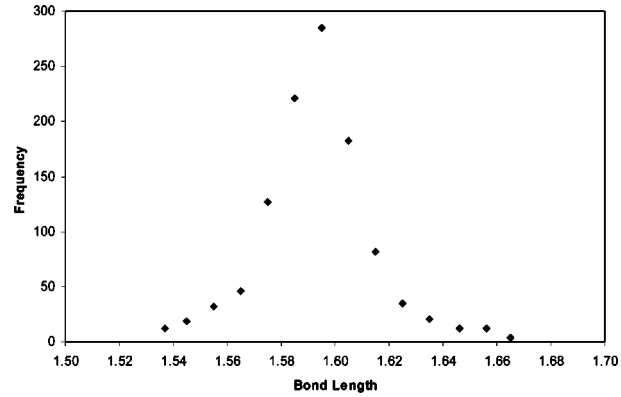

Figure 1. Si−O Bond length (in Å) distribution for pure silica zeolite structures collected at temperatures between −100 and 25 °C. The frequency peak at the grand mean value of 1.597 Å is clearly visible.

$$d = 1.579 + 0.015\langle \mathrm{CN}(O)\rangle \quad (1)$$

Where d is the Si−O distance and $\langle \mathrm{CN}(O)\rangle$ is the coordination number of oxygen. Since all of the oxygen atoms in PSZ are 2-coordinate, it is reasonable to take this as a starting point. Liebau also points out that Si−O bonds in which the oxygen is linked to a second silicon atom are slightly weaker than Si−O−M (where M = Na, Ca, K, etc.) linkages. The fact that our grand mean value is shorter than the previously accepted value by more than 0.01 Å seems to contradict this; however, because the standard deviation in our value is 0.026, which means that the two values are not significantly different, all we can say is that the findings of our analysis broadly agree with those of Liebau. This is exactly what we would expect.

The shortest bond from a structure collected at room temperature is 1.540(9) Å in the calcined MCM-35 structure.[49] This appears to be a reliable value (no restraints were used in the refinement and the estimated standard deviation (esd) is small) and several other structures have bonds of similar lengths. At the other end of the range, we find several structures with bond lengths of around 1.70 Å.

For calcined materials, the ranges are smaller (1.540(9)−1.672(6) Å), with a narrower range again, 1.56(2)−1.65(2) Å, for single crystal data, reflecting their more regular overall structure (obviously the range for the as-made materials is the same as the overall range). This suggests that there may be additional distorting effects from the SDA, which are lost on its removal. An interesting case here is that of SSZ-35, which changes from monoclinic to triclinic symmetry on calcination.[31] The structure is very similar to that of ITQ-4, which maintains its symmetry on calcination. However, the low-symmetry topology has been calculated to be 5 kJ mol^{-1} more stable than the high-symmetry form.[86] Reference 31 also reports the framework structure of SSZ-35 determined from synchrotron single-crystal XRD data. Because of the

(75) Spek, A.L. J. *Appl. Crystallogr.* **2003**, *36*, 7–13.
(76) The ITQ-n and SSZ-n series encompass a huge range of silicate, aluminosilicate, and other open framework materials prepared in several different ways. Many of the references in this paper cover materials in these series (10, 14, 27−36, 45, 50, 53−57), as do the reviews of refs 4−6. References within these papers will lead the curious reader to many further examples of these remarkable series.
(77) Cernik, R. J.; Clegg, W.; Catlow, C. R. A.; Bushnell-Wye, G.; Flaherty, J. V.; Greaves, G. N.; Hamichi, H.; Burrows, I.; Taylor, D. J.; Teat, S. J. *J. Synchrotron Radiat.* **1997**, *4*, 279–286.
(78) Brown, G. E.; Gibbs, G. V.; Ribbe, P. H. *Am. Mineral.* **1969**, *54*, 1044–1061.

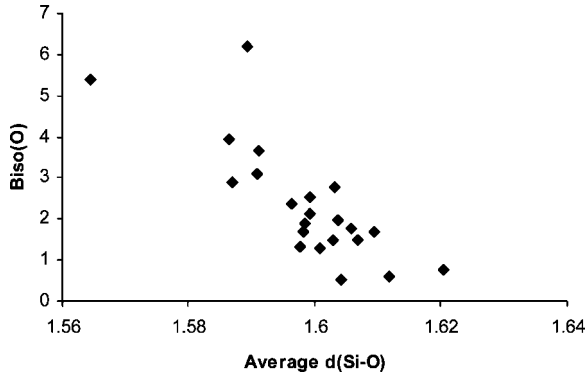

Figure 2. Plot of average Si−O distance (Å) against thermal disorder as expressed by the average B_{iso} value for the oxygen atoms in the structure. B_{iso} is derived from the isotropic temperature factor U_{iso}, which was refined in very few of the powder data sets; therefore, only single-crystal data collected between −100 and 25 °C have been used. The bond length generally decreases with increasing thermal disorder.

disorder of the SDA, the *R* factors for this structure did not meet the acceptability criterion for this study; however, a further refinement of the same data using the program SQUEEZE from the PLATON[76] crystallographic software suite to remove nonframework peaks from the Fourier map gave $R = 0.0607$ for observed data ($F_o > 4\sigma F$) and 0.0768 for all data.[68] The electron density removed from the Fourier map using SQUEEZE is calculated to be equivalent to 51 electrons. The template used in the synthesis (*N*,*N*-dimethyl-6-azonium-1,3,3-trimethylbicyclo(3.2.1)octane) has 103 electrons, which indicates that there is one template molecule for every two asymmetric units of the structure.

The variable-temperature investigation of Bull and co-workers is of interest in that it reveals that pure silica ferrierite actually exists in both primitive and body-centered forms depending on the temperature with the transition from low to high symmetry occurring at 400 K. The study also shows that negative thermal expansion occurs in this system, i.e., the material contracts as the temperature increases![28] Negative thermal expansion has been observed in the pure silica forms of zeolite-Y,[79] ferrierite,[28] MCM-22(ITQ-1, SSZ-25), ITQ-3, SSZ-23,[80] chabazite,[81] ITQ-4,[32,81] ITQ-7, and SSZ-35(ITQ-9, MU26).[82] Computer simulations predict that many other zeolites should have this odd property.[83,84] Negative thermal expansion in zeolites has been studied by both powder[79,80] and single-crystal[28,34] XRD as well as by neutron diffraction[81,82] and, recently, pair distribution function analysis.[85]

There seems to be some correlation between the bond length and thermal disorder as represented by the B_{iso} parameter for these structures as was found by Liebau for dense silicas (Figure 2). It seems that the effect of thermal disorder outweighs any tendency for the bonds to extend at high temperature. This can be used to adjust bond lengths for thermal disorder, and an equation is proposed by Liebau based on regression analysis of 85 bonds from 25 structures (see eq 2).

$$d_{\text{corrected}} = d + 0.007B(\text{O}) \tag{2}$$

where *d* is the Si−O distance and *B* is the thermal parameter.

Bull and co-workers' study of negative thermal expansion in ferierrite[28] shows that its average bond length decreases from around 1.600 Å at 150 K to around 1.585 Å at just over 500 K. Bond shortening with temperature is also observed in a variable-temperature study of ITQ-4 by Villaescusa et al.[34] Using a more recent formula (eq 3)[87] that compensates for the thermal disorder in a slightly more sophisticated manner, the authors show that the bond lengths do in fact increase (fractionally) with temperature.

$$d^2_{\text{corrected}} = d^2 + \frac{3}{8}\pi^2[B_{\text{eq}}(\text{O}) - B_{\text{eq}}(\text{Si})] \tag{3}$$

It seems that the difference between the PSZ and dense silicate phases in terms of the Si−O bond lengths is quite small. The negative thermal expansion properties, however, point to significant differences between porous and dense silicas, which may be explained with analysis of the bond angles involved. An interesting observation here comes from the study of the compression mechanism of trioxane sodalite by Fuetterer et al.[64] The bond lengths in this study vary only a little (from 1.599(2) to 1.615(7) Å) over a wide range of pressure (0.0001 to 1.28 GPa) and indeed increase with pressure, whereas the lattice constant shows a significant reduction from 8.839 to 8.745 Å. The proposed contraction mechanism is based on a tilting motion of rigid tetrahedra with the Si−O−Si angles decreasing from 155.3(2) to 147(1)° and the tilt angle increasing from 8.4(2) to 14.7(8)°. The authors discuss the theory that this tilting allows the framework to incorporate organic guest molecules. It has also been used to explain the thermal expansion of sodalite.[88]

O−Si−O Angle. The ideal tetrahedral angle is 109.5°. The grand mean average for our set of PSZ structures is 109.5 ± 2.6°. The standard deviation shows that the range of values for these angles is wide. Liebau gives a range of 98 to 122°, we have found an upper limit of 129.2(16)° and a smallest angle of 96.8(8)°. The most common value (Figure 3.) is in fact exactly 110°.

The largest angle is found in the ITQ-24 structure; however, NMR evidence suggests that (although the Rietveld refinement converged without restraints on the framework bonds and angles) the true structure probably has lower symmetry.[41] Large esds in the atomic parameters also suggest that this is not the best of structures. Most of the extreme

(79) Hochgräfe, M.; Marler, B.; Gies, H.; Fyfe, C. A.; Feng, Y; Grondey, H.; Kokotailo, G. T. *Z. Kristallogr.* **1996**, *211*, 221–227.
(80) Attfield, M. P.; Sleight, A. W. *Chem. Mater.* **1998**, *10*, 2013.
(81) Woodcock, D. A.; Lightfoot, P.; Wright, P. A.; Villaescusa, L. A.; Díaz-Cabañas, M.-J.; Camblor, M. A. *J.Mater. Chem.* **1999**, *9*, 349–351.
(82) Woodcock, D. A.; Lightfoot, P.; Wright, P. A.; Villaescusa, L. A.; Díaz-Cabañas, M.-J.; Camblor, M. A.; Engberg, D. *Chem. Mater.* **1999**, *11*, 2508–2514.
(83) Lightfoot, P.; Woodcock, D. A.; Maple, M. J.; Villaescusa, L. A.; Wright, P. A. *J. Mater. Chem.* **2001**, *11*, 212–216.
(84) Tschaufeser, P.; Parker, S. C. *J. Phys. Chem.* **1995**, *99*, 10609–10615.
(85) Gale, J. D. *J. Phys. Chem. B* **1998**, *102*, 5423–5431.
(86) Martínez-Iñesta, M. M.; Lobo, R. F. *J. Phys. Chem. B* **2005**, *109*, 9389–9396.
(87) Villaescusa, L. A.; Barrett, P. A.; Camblor, M. A. *Chem. Commun.* **1998**, 2329–2330.
(88) Downs, R. T.; Gibbs, G. V.; Bartelmehs, K. L.; Boisen, M. B., Jr *Am. Mineral.* **1992**, *77*, 751–757.

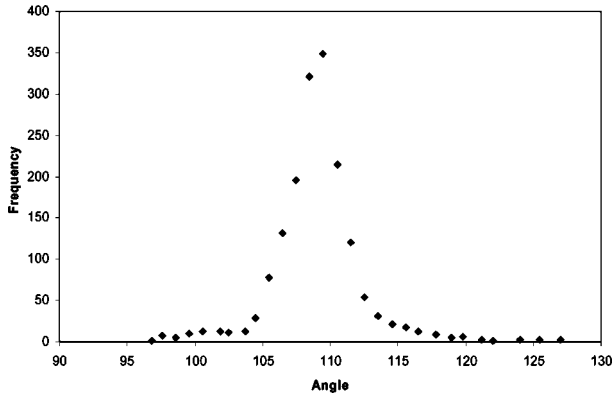

Figure 3. O−Si−O bond angle (deg) distribution for pure silica zeolites.

O−Si−O angles found in as-made PSZ crystal structures are associated with $SiO_{4/2}$ sites distorted toward trigonal bipyramidal geometry by the presence of fluorine. These angles are excluded from our main analysis but the distortion is discussed below. In the analyzed structures, the smallest angle is 96.8(8)° in calcined SSZ-24. The latter is rather unusual in having a wider range of O−Si−O angles in the calcined than the as-made form because the calcined structure contains a disordered oxygen atom modeled as two separate sites. The Rietveld refinements in each case are of similar quality (no restraints used, similar esds and R_{wp}s). The fact that calcined and as-made materials have a similar range of O−Si−O angles is expected, as SiO_4 tetrahedra are recognized as fairly rigid units. In support of this, the range of calculated lattice energies in PSZ is quite narrow, between 5 and 20 kJ mol^{-1} greater than that of quartz.[89,70] The slight shift toward an ideal tetrahedral angle from as made to calcined structures is shown in Figure 4.

Fluorine. Mineralizers, such as fluoride ions, added to the reaction mixtures in the correct quantities are often vital for crystallization of the desired molecular sieve products. Fluoride in particular has recently been an extremely useful mineralizer in metallophosphates[90–93] as well as silicate synthesis. In addition to helping solubilize the starting materials under the reaction conditions, there is evidence that fluoride itself can play a structure-directing role.[94–96]

When fluorine is present in the structure, the angles around the $SiO_{4/2}$ tetrahedra are influenced by the additional coordination of fluorine atoms. The fluorine atom is often linked to a four ring and in all structures determined to date (excepting ZSM-23, which was treated with ammonium fluoride and steamed at 1023 K rather than actually being synthesized in the presence of fluoride) enclosed in a small cage. Recent simulations by Pulido et al. have shown how the location of the fluoride depends on electrostatic interactions with the SDA in several as made PSZ.[97] Eight environments have been unequivocally determined from diffraction data, and these are shown in Table 2.

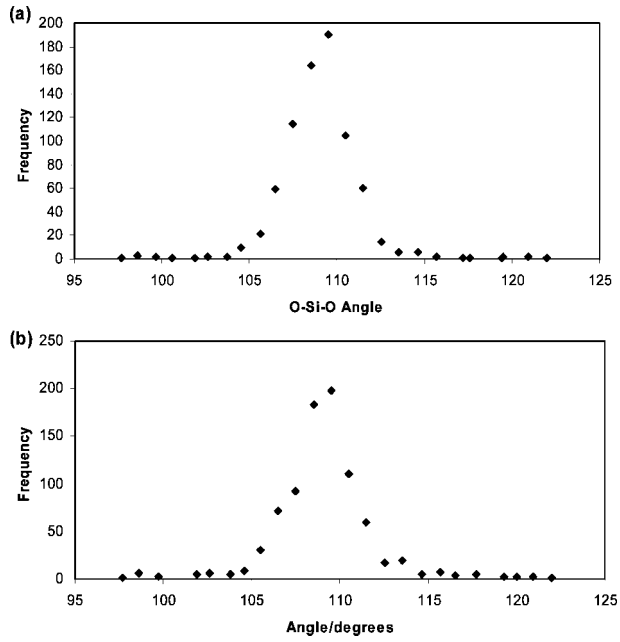

Figure 4. O−Si−O Bond angle (deg) distributions for (a) as-made and (b) calcined pure silica zeolites. The most frequently observed value in b is around 109°; in a, it is about110°.

Table 2. Cage Environments and Si−F Bond Lengths for Fluorine in PSZ Type Structures.[a]

structure	*d*(Si−F) (Å)	cage type
octadecasil	2.632(29)	$[4^6]$
SSZ-55	1.987(19)	$[4^66^2]$
SSZ-55	1.899(19)	$[4^66^2]$
chabazite	2.02(2)	$[4^66^2]$
siliceous ferrierite	2.01(2)	$[5^4]$
ITQ-4	1.914(11)	$[4^35^26^1]$
ITQ-13	2.632(6)	$[4^6]$
ITQ-13	2.631(5)	$[4^6]$
ITQ-13	1.76(3)[b]	$[4^15^4]$
silicalite, ZSM-5	1.915(3)	$[4^15^26^2]$
nonasil	1.836(7)	$[4^15^46^2]$
SSZ-35, ITQ-9, MU-26	1.868(8)	$[4^15^26^2]$
SSZ-35, ITQ-9, MU-26	1.983(6)	$[4^15^26^2]$
SSZ-35, ITQ-9, MU-26	1.745(6)	$[4^15^26^2]$
SSZ-23	1.96(3)	$[4^35^4]$
SSZ-23	1.95(2)	$[4^35^4]$
SSZ-23	1.937(14)	$[4^35^4]$

[a] The cages are described in terms of the number *m* of rings with *n* Si−O−Si edges: $[n^m n'^{m'} \ldots]$. [b] Constrained to a distance determined from NMR data.

The O-Si-O angles around the Si atoms to which fluoride is coordinated are distorted away from tetrahedral toward trigonal bipyramidal geometry. The Si-F bond length depends on the type of cage in which the F atom sits and this also influences the degree of distortion of the O-Si-O angles away from 109.5° (Figure 5).

Generally, the longer the Si−F bond, the smaller the distortions in the tetrahedral angles; however, there are some

(89) Henson, N. J.; Cheetham, A. K.; Gale, J. D. *Chem. Mater.* **1994**, *6*, 1647–1650.
(90) Morris, R. E.; Burton, A.; Bull, L. M.; Zones, S. I. *Chem. Mater.* **2004**, *16*, 2844–2851.
(91) Villaescusa, L. A.; Lightfoot, P.; Morris, R. E. *Chem. Commun.* **2002**, 2220–2221.
(92) Wragg, D. S.; Morris, R. E. *J.Am. Chem. Soc.* **2000**, *122*, 11246–11247.
(93) Wragg, D. S.; Slawin, A. M. Z.; Morris, R. E. *J. Mater. Chem* **2001**, *11*, 1850–1857.
(94) Parnham, E. R.; Wheatley, P. S.; Morris, R. E. *Chem. Commun.* **2006**, 380–382.
(95) Cooper, E. R.; Andrews, C. D.; Wheatley, P. S.; Webb, P. B.; Wormald, P.; Morris, R. E. *Nature* **2004**, *430*, 1012–1016.
(96) Parnham, E. R.; Wheatley, P. S.; Morris, R. E. *Chem. Commun.* **2006**, 380–382.
(97) Pulido, A.; Corma, A.; Sastre, G. *J. Phys. Chem. B* **2006**, *110*, 23951–23961.

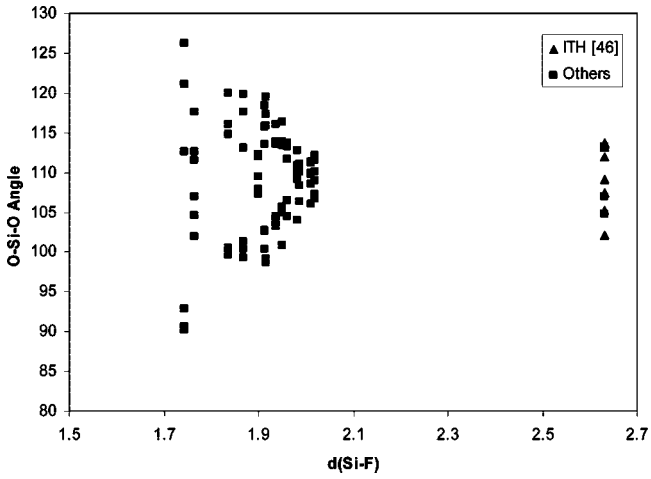

Figure 5. Distortion of O−Si−O bond angles (deg) increases with decreasing Si−F bond length. The fluorine in the [4^6] cage of ITH is marked separately.

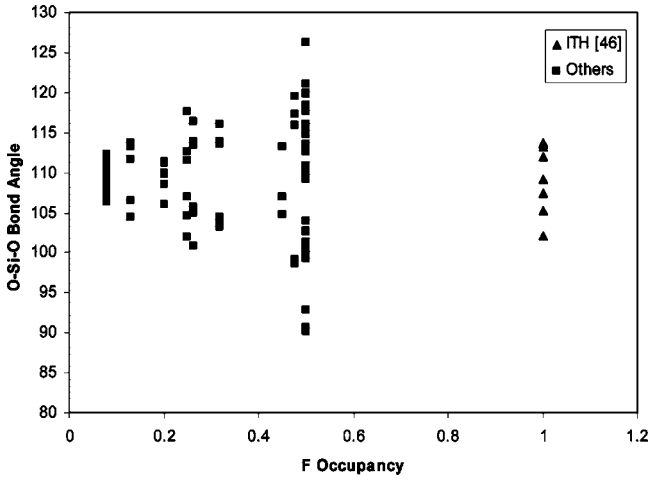

Figure 6. O−Si−O angle (deg) distortion generally decreases with F occupancy. The fluorine in the [4^6] cage of ITH is marked separately.

apparent anomalies; for example, ITQ-13 with a Si−F length of 1.76 Å has a spread of bond angles similar to those in SSZ-23, which has a Si−F bond length of 1.95 Å. Often, the fluoride sites in PSZ are not fully occupied. A plot of F occupancy against distortion shows that the distortion increases with the likelihood of finding an F atom on the site (Figure 6). An exception to this comes from the fact that the only 100% occupied F site is in the [4^6] cage of ITQ-13; this has a very long Si-F distance (2.631 Å), so as we have seen above, the fluorine has very little influence on the O−Si−O angles.

Combining the two measures by plotting the O−Si−O angle against the Si−F distance divided by occupancy (assuming that reducing the occupancy has the same effect as extending the bond) gives a graph that shows a reduction in tetrahedral distortion with increasing bond length and reducing occupancy (Figure 7). Again, however, the 100% occupied fluoride in the [4^6] cage of ITQ-13 (**ITH**) does not fit the pattern.

Fluoride is thought to have an important role in the synthesis mechanisms of PSZ, acting as a template for the formation of small cages (it is usually found close to a four-ring window[6]), and it has been postulated that small

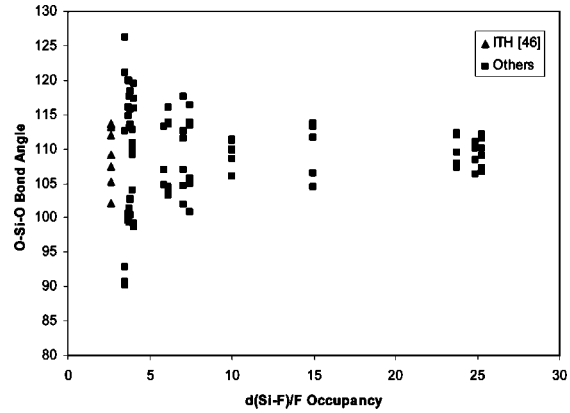

Figure 7. Distortion of the O−Si−O angles related to Si−O distance (Å) and occupancy of the fluorine site. The fluorine in the [4^6] cage of ITQ-13 is marked separately.

differences in the ordering of the fluorine atoms may indicate different mechanisms for the formation of SSZ-35 and ITQ-4, which have very similar small cage units.[33] In this case, the ordering of the F atoms in ITQ-4 could not be clearly determined by X-ray diffraction until synchrotron data were collected. The positioning of F atoms in one side of the [$4^3 5^2 6^1$] cage leads to the crystal structure becoming non-centrosymmetric (space group *Im*) despite the fact that the PSZ framework itself is centrosymmetric (spacegroup *I*2/*m* for the calcined version). It is thought that the ordering of the F atoms in half of the available cages leads in turn to ordering of the organic SDA, which is found in only one orientation (Figure 8).

In fact, NMR data shows that a similar ordering occurs in SSZ-35.[67] The ordering could not be resolved by XRD but by building two $SiO_{4/2}$ tetrahedra with 50% occupancy into the model for the Si3 site, we found that a refinement with the Si−F distances indicated by NMR was gave improved *R* factors. This led to the unusual Si−O bond lengths and angles discussed above.

At first glance, it might seem rather odd that these structures are even included in this study; however ,we feel that the influence of fluoride in the structures of silica frameworks synthesized in its presence is extremely significant. The structural significance of fluoride was often missed by early researchers in this field.

Si−O−Si Angle. The bond angles around the oxygen atoms in the PSZ structures are very flexible. This makes them important in the explanation of negative thermal expansion, compression, and the formation of open frameworks. The range of values for this angle found in the PSZs (133.6(4) to 180(1)°) reflects this flexibility, with the average value of 154 ± 9° for all structures also being somewhat different from the most frequent value in the distribution graph (Figure 9). The shape of the distribution graph is similar to that described by Liebau (who cites work by Baur[98]) but has its main peak at 148° with a shoulder at around 153°. These fit quite well with Liebau's values from a sample of 39 bond angles in well-defined silica polymorphs, which give a maximum at about 147° and a shoulder at about 157°. Our graph also shows a shoulder at 141° and a peak

(98) Baur, W. H. *Acta Crystallogr., Sect. B* **1980**, *36*, 2198–2202.

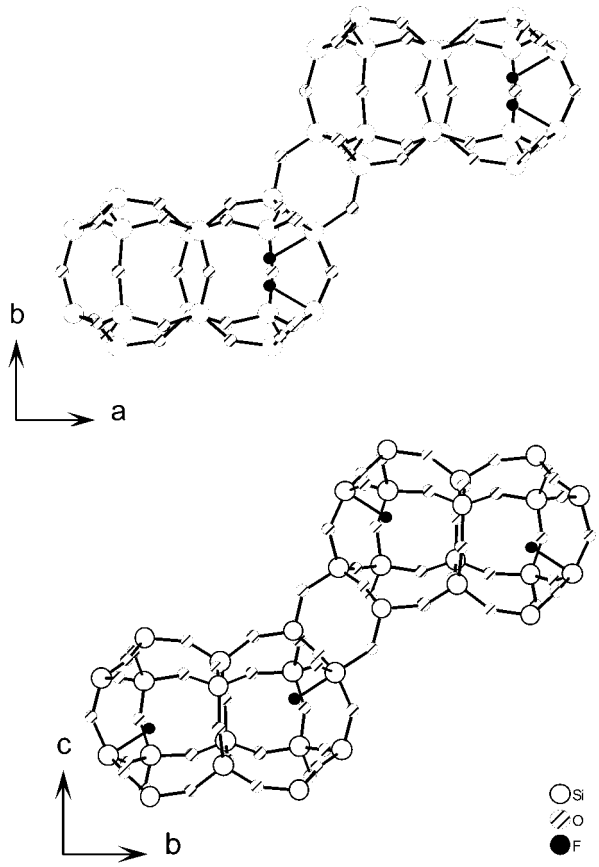

Figure 8. Differences in fluoride ordering between pure silica zeolites ITQ-4 (top) and SSZ-35 (bottom). In ITQ-4, the fluorides (black spheres) form a noncentrosymmetric arrangement, whereas in SSZ-35, the arrangement is centrosymmetric. In both cases, the fluoride ion occupancy is 50%. In ITQ-4, the disorder is dynamic at room temperature, whereas in SSZ-35, it is static.

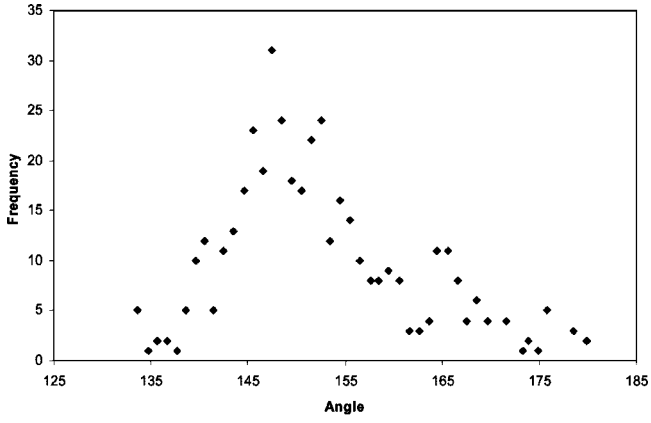

Figure 9. Si−O−Si angle (deg°) distribution for pure silica zeolites.

at 165°: could these be angles that are of some significance in the formation of open frameworks?

The average value of the Si−O−Si angle for each of the analyzed structures is given in Table 3. The figures take into account the multiplicities of the oxygen sites in the crystal structure, and the standard deviations give an idea of how variable the angles in each structure are. One might expect that the calcined structures would have the smallest angle ranges, but this is not the case (although the two smallest standard deviations are in calcined structures); the calcined and as-made structures both exhibit a wide range of angles.

In early structure determinations for silicas, 180° Si−O−Si angles were common because of oxygen atoms apparently residing on special crystallographic positions that forced the angles to 180° with their symmetry. Many of these results were due to incorrect structures as is noted by Cheetham and co-workers in their paper on the structure of pure silica ferierrite.[27] This material was, as discussed above, thought to have *Immm* symmetry but is in fact better described in *Pmmn* at room temperature. The body-centered structure features 180° Si−O−Si angles forced by symmetry but the primitive version does not. In the up to date structures analyzed here, some 180° angles still remain in dodecasil-1H. In addition to this, dodecasil-3c (pure silica ZSM-39) and silicalite (pure silica ZSM-5 with and without fluorine) have angles above 175° that are not restricted by symmetry. Several of these structures exhibit wide ranges of the Si−O−Si angle (see Table 3); however, in dodecasil-1H, the standard deviation is only ± 7.8° from a mean value of 170.6°.

Liebau[7] suggests that most 180° angles in silicates are caused by unresolved static disorder, presenting evidence that the thermal parameters of oxygen atoms with Si−O−Si angles of 180° are mostly rather larger than average for the structures. Because diffraction cannot differentiate between static and dynamic disorder, the presence of two O sites on either side of the special position would be indicated by a large thermal ellipsoid. In some dense phases, especially that of coesite (a silicate prepared at high temperature), the oxygen on the special position does not have an unusually large displacement parameter. In this material, the thermal parameter of the O with 180° bond angles increases rapidly with increasing pressure, whereas those of the other oxygen atoms decrease. The authors believe this is due to the symmetric Si−O−Si bond being destabilized with pressure.[99] Dodecasil-1H has a 180(0)° bond angle from Si4−O7−Si4. O7 does have a large thermal parameter, indicating that there may be some static disorder in the framework; however, it has by no means the largest atomic displacement ellipsoid in the structure. The authors suggest that there is in fact a large amount of unresolved disorder throughout the structure; this could explain the very high mean Si−O−Si angle.[23] The work of Evans and co-workers on complex phosphate materials gives another insight here. Many of the structures they have studied appear initially to have simple asymmetric units that build up into structures with 180° metal–oxygen−phosphorus (M−O−P) angles and large oxygen displacement ellipsoids. On closer analysis, using simulated annealing techniques, they are found to have very large asymmetric units (441 independent atoms in the case of $Mo_2P_4O_{15}$) with well-ordered structures, no 180° M−O−P angles, and small thermal parameters for the oxygen atoms.[100] Could a similar level of complexity be hiding in these curious PSZ structures? It would fit with the way in which the 180° angles in siliceous ferierrite disappear when the correct structural model is used.[27] It seems reasonable to assume that the 180° angles in PSZ are due to unresolved disorder or structural complexity rather than unusual bonding properties.

(99) Levien, L; Prewitt, C. T. *Am. Mineral.* **1981**, *66*, 324–333.

Table 3. Mean Si−O−Si Angles for PSZ, Adjusted for the Multiplicity of the Oxygen Sites

material	structure code	calcination status	data type	average Si−O−Si angle (deg)	standard deviation	ref
SSZ-24	**AFI**	calcined	P	151.3	8.9	11
SSZ-24	**AFI**	as-made	P	152.7	13.5	11
octadecasil	**AST**	as-made	SC	142.8	4.0	12
SSZ-55	**ATS**	as-made	SC	147.1	3.4	13
chabazite	**CHA**	calcined	P	148.0	2.0	18
chabazite	**CHA**	as-made	SC	146.8	3.7	19
chabazite	**CHA**	calcined	SC	148.5	1.4	20
dodecasil-1H	**DOH**	as-made	SC	170.6	7.8	22
zeolite-Y	**FAU**	calcined	P	143.7	4.8	25
ferrierite	**FER**	as-made	SC	153.3	8.2	26
ferrierite	**FER**	calcined	SC	152.6	8.3	19
ferrierite	**FER**	as-made	SC	154.2	6.3	27
ITQ-4	**IFR**	calcined	P	149.7	6.8	29
ITQ-4	**IFR**	calcined	P	149.1	8.9	30
ITQ-4	**IFR**	as-made	SC	146.3	8.4	31,32
ITQ-4	**IFR**	calcined	SC	145.9	6.4	33
ITQ-7	**ISV**	calcined	P	150.8	9.1	35
ITQ-13	**ITH**	as-made	SC	150.0	9.4	37
ITQ-24	**IWR**	calcined	P	150.5	11.5	41
ITQ-29	**LTA**	calcined	P	153.3	4.6	42
ZSM-11	**MEL**	calcined	P	153.6	8.0	43
ZSM-11	**MEL**	calcined	P	152.7	7.6	44
ZSM-11	**MEL**	as-made	SC	153.8	7.4	45,46
ZSM-5	**MFI**	as-made	SC	156.0	9.1	47
ZSM-5	**MFI**	as-made	SC	153.7	10.4	48
MCM-35	**MTF**	calcined	P	154.5	10.8	49
ZSM-39	**MTN**	as-made	SC	152.7	7.5	50
ZSM-39	**MTN**	as-made	SC	162.7	10.1	51
ZSM-39	**MTN**	as-made	SC	163.6	10.5	52
ZSM-12	**MTW**	calcined	P	150.0	6.8	54
ZSM-12	**MTW**	calcined	P	149.1	7.1	55
nonasil	**NON**	as-made	SC	149.9	7.1	57
RUB-10	**RUT**	as-made	P	154.1	6.3	60
sigma-2	**SGT**	calcined	P	154.8	10.4	63
sodalite	**SOD**	as-made	P	155.2	0.2[a]	64
sodalite	**SOD**	as-made	SC	159.7	0.2[a]	65
sodalite	**SOD**	as-made	P	159.6	0.1[a]	65
SSZ-35	**STF**	as-made	SC	150.8	11.0	67
SSZ-35	**STF**	as-made	SC	151.4	10.2	68
SSZ-23	**STT**	as-made	SC	150.2	8.8	69
theta-1	**TON**	calcined	SC	150.5	4.0	71

[a] These figures are refinement esds, as there is only one Si−O−Si angle in the structure.

Variable-temperature studies on pure silica ferierrite show the equivalent bond angles in the low- and high-temperature forms quickly change from around 170 to 180° at 400 K when the primitive to body-centered phase change occurs. Below the transition temperature, a slight increase in the bond angle with temperature (163 to 170°) is observed. The negative thermal expansion that occurs below the phase transition point is explained by the reduction of some of the Si−O−Si bond angles, leading to decreases in the Si−Si distances. This is similar to the explanation used by Fuetterer et al.[64] for the compression of trioxane sodalite, but it is not the only mechanism. In ITQ-4, for example, one of the Si–Si distances that decreases the most is parallel with a crystallographic axis that extends with temperature. The negative thermal expansion is explained by twisting of the $SiO_{4/2}$ tetrahedra and entire ring and cage units. Cage-based sections of the structure remain fairly rigid or expand slightly, whereas ring units are more flexible and able to contract. In fact, it seems that the cage sections (columns of $[4^3 5^2 6^1]$ cages in IFR) behave almost like dense silicas when heated.[34]

The structural diversity of PSZ is probably based on the wide range of Si−O−Si angles that are possible. The presence of local maxima at 141 and 165° in the distribution graph, which are not noted in previous analyses of predominantly dense phases, suggests that these angles may be characteristic of open framework silicas. It seems likely that tilting of rigid tetrahedra with flexible Si−O−Si angles allows the formation of pores and cages. These then behave in very different ways when heated.

Conclusions

We can draw several conclusions from this analysis on the nature of PSZ:

(1) The Si−O bond length ranges from 1.54 to 1.67 Å, with a grand mean value of 1.594 ± 0.027 Å.

(2) The O−Si−O angle ranges from 129.2 to 96.8°, with a mean value of 109.5 ± 2.6° and a most common value of 110°.

(3) In structures containing fluorine, the O−Si−O bond angles are distorted away from tetrahedral and toward trigonal bipyramidal geometry as the Si−F bond length decreases and the occupancy of the F site increases.

(4) The Si−O−Si bond angle can adopt a wide range of values from 133.6 to 180° ,with the most common value being 148°, slightly less than the mean value of 154 ± 9°.

(100) Lister, S. E.; Radosavljevic Evans, I; Howard, J. A. K.; Coelho, A; Evans, J. S. O. *J. Chem. Soc., Chem. Commun.* **2004**, 2540–2541.

(5) Si−O−Si bond angles of 141 and 166° are relatively more common in PSZ than in other silicas.

(6) The flexibility of Si−O−Si bonds probably allows for the formation of the many structural motifs in PSZ.

(7) 180° Si−O−Si angles are probably due to unresolved disorder or structural complexity.

The combination of these properties leads to a remarkable set of materials.

Acknowledgment. The authors thank Professor Reinhard Fischer for his extremely useful comments and suggestions on the original manuscript. R.E.M. and D.S.W. thank the EPSRC for funding. We also acknowledge use of the UK chemical database service.

Supporting Information Available: Crystallographic information for STF with template electron density removed using the SQUEEZE[74] program (CIF). This material is available free of charge via the Internet at http://pubs.acs.org.

CM071824J